Image-based iterative compensation of motion artifacts in computed tomography

Colas Schretter[a)]
Philips Research Europe, Weisshausstrasse 2, 52066 Aachen, Germany and Otto-von-Guericke University, Universitätsplatz 2, 39016 Magdeburg, Germany

Georg Rose
Otto-von-Guericke University, Universitätsplatz 2, 39016 Magdeburg, Germany

Matthias Bertram
Philips Research Europe, Weisshausstrasse 2, 52066 Aachen, Germany

(Received 8 May 2009; revised 16 September 2009; accepted for publication 16 September 2009; published 22 October 2009)

Purpose: This article presents an iterative method for compensation of motion artifacts for slowly rotating computed tomography (CT) systems. Patient's motion introduces inconsistencies among projections and yields severe reconstruction artifacts for free-breathing acquisitions. Streaks and doubling of structures can appear and the resolution is limited by strong blurring.
Methods: The rationale of the proposed motion compensation method is to iteratively correct the reconstructed image by first decomposing the perceived motion in projection space, then reconstructing the motion artifacts in image space, and finally subtracting the artifacts from an initial image. The initial image is reconstructed from the acquired data and might contain motion blur artifacts but, nevertheless, is considered as a reference for estimating the reconstruction artifacts.
Results: Qualitative and quantitative figures are shown for experiments based on numerically simulated projections of a sequence of clinical images resulting from a respiratory-gated helical CT acquisition. The border of the diaphragm becomes progressively sharper and the contrast improves for small structures in the lungs.
Conclusions: The originality of the technique stems from the fact that the patient motion is not explicitly estimated but the motion artifacts are reconstructed in image space. This approach could provide sharp static anatomical images on interventional C-arm systems or on slowly rotating X-ray equipments in radiotherapy.
[DOI: 10.1118/1.3244035]

Key words: X-ray tomography, image reconstruction, motion compensation, iterative methods

I. INTRODUCTION

X-ray transmission computed tomography (CT) reconstructs a volumetric attenuation image from several radiographies of a static object. Digital radiographs are taken at different orientations during a sequential data acquisition phase. Raw data contains measured intensities, proportional to the number of photons that were not absorbed during their transport through the object lying between the focus point and the detector. Knowing the initial emitted intensity, the input data are converted to digital tomographic projections that sample line integrals through the object.

If the observed object remains static during the acquisition, then the projections are *consistent* and a reconstruction from the line integrals is possible in the field of view (FOV).[1] In medical applications, especially with slow cone-beam CT devices,[2] the observed object is alive and is therefore never completely static. With open-gantry CT systems, a full rotation can last for several seconds up to about one minute, and often the patient is unable to hold his breath during the whole acquisition. Therefore, the motion of organs during the exposition has to be taken into account.

If breathing occurs during the acquisition, the diaphragm contracts and pulls down the organs to enlarge the thoracic volume. The organ motion is space variant, roughly periodic, and mainly axial. In particular, organs can move inside and outside the FOV during the acquisition. Therefore, the measured line integrals are strongly biased and the input projections are *inconsistent*.

Early approaches to avoid data inconsistencies have been to use a fast rotation speed of the gantry[3] or to adapt the rotation speed[4,5] for each specific imaging application. However, the acquisition time on radiotherapy and interventional C-arm systems is slower than that on diagnostic closed-gantry CT scanners and the inconsistency of the acquired data is an unavoidable problem. Prospective respiratory gating schemes can be used to acquire only projections that correspond to a given motion state,[6] while retrospective gating allows the reconstruction of an image for each motion state of the breathing cycle.[7] As a drawback, methods based on gating make the strong assumption that the patient motion is periodic.

Another approach is incorporating a description of the motion in the image reconstruction algorithm. Several exact motion-compensated reconstruction algorithms of increasing

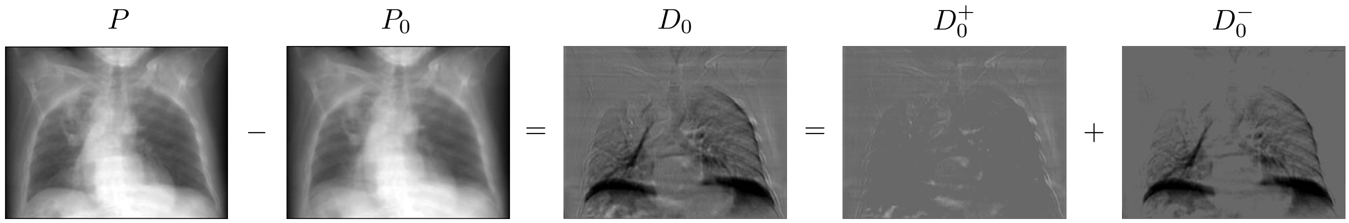

FIG. 1. Example of decomposition of line integral differences (D_0) between an acquired projection (P) and a reference projection (P_0) computed for the first iteration. Either the positive (D_0^+) or negative (D_0^-) parts of differences (D_0) will be reconstructed to estimate the motion artifacts in image space. The consequences of motion are very apparent at the border of the diaphragm. In (D_0), (D_0^+), and (D_0^-), gray corresponds to zero, while brighter and darker values correspond to negative and positive differences, respectively.

complexity have been proposed for various classes of deformations.[8–11] However, the motion information needs to be measured or estimated from the data before reconstruction. Many authors proposed to use *a priori* information to estimate the patient motion, such as a gated 4D dynamic image[12] or a diagnostic 3D static image.[13]

Alternative solutions based on precorrection of input projection data exist to handle nonperiodic motion in CT. The correction is applied prior to reconstruction by resampling the data after estimating the motion in projection space[14] or by modifying the values of line integrals to ensure data consistency conditions. Therefore, those methods allow using standard image reconstruction algorithms; however, they are dedicated to capture only smooth motion[15] or a limited class of deformations such as global translations[16] or rigid body motion.[17] Furthermore, the resampling step introduces some additional blurring and aliasing artifacts in the projection data.[18]

In contrast to the existing approaches, this work proposes an iterative motion compensation technique that leaves the input data untouched but aims to correct the output reconstructed image. The advantage is that the algorithm provides very quickly an early reconstructed image and the image quality of this initial reconstruction is progressively improving from iteration to iteration. The instant feedback feature is crucial for using CT protocols on C-arm systems during interventions and is helpful for patient positioning in radiotherapy.[19]

The rationale of the method is to correct the reconstructed image by first extracting the motion artifacts in projection space, then reconstructing the artifacts in image space, and finally subtracting the artifacts from the original reconstruction without any motion compensation. This technical approach was inspired by the two-pass algorithm for cone-beam reconstruction proposed by Hsieh,[20] while the principle of motion detection from the difference between line integrals was first proposed by Lin[21] and studied further by Linney and Gregson.[22]

II. METHOD

The iterative nature of the technique exploits the fact that the forward projection is the inverse of the image reconstruction. Therefore, if one samples line integrals through the reconstructed image, then the resulting reference projections should match the acquired projections. However, if the acquired projections are inconsistent, the reconstructed image will be corrupted by motion artifacts. In this case, sampled reference projections will not match the acquired projections.

The iterative image correction works as follows. First, difference projections are computed by subtracting reference projections from the acquired projections and the differences are decomposed into positive and negative parts. Then, the artifacts are reconstructed in image space from either the positive or the negative part of the decomposition. Finally, the artifacts are subtracted from the initial image, improving

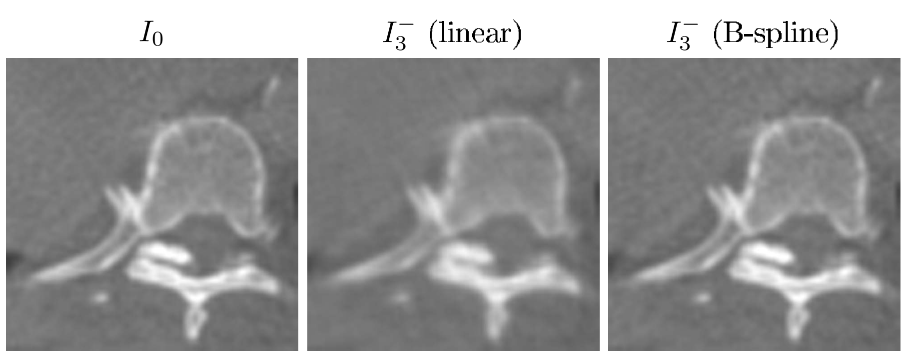

FIG. 2. Close-up views of 64×64 pixels showing the spine in a transversal slice of the initial FBP image (I_0) and the corrected images (I_3^-). The spine is a mainly static region and is already sharply reconstructed in the initial FBP image. Strong blurring is introduced when using linear interpolation while the sharpness is preserved with cubic B-spline interpolation. Image interpolation is used for sampling forward projections from volumetric digital images.

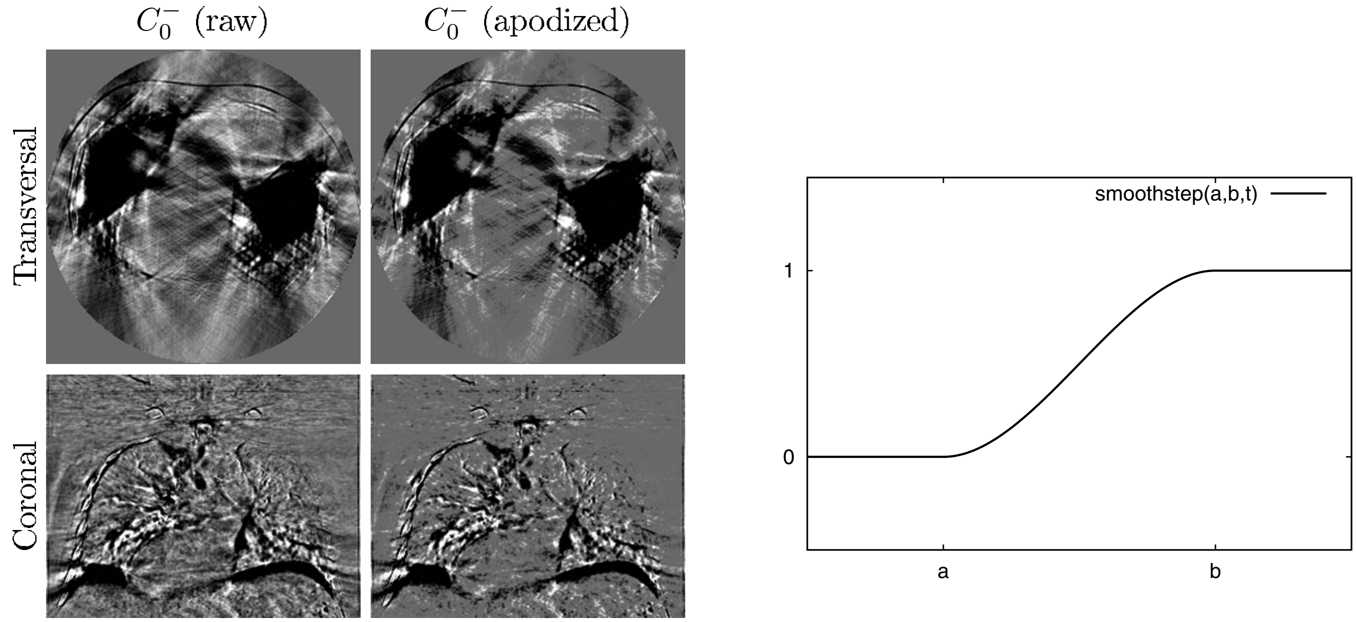

FIG. 3. Impact of the apodization on the correction image C_0^-, computed from the negative part of line integral differences, at the third iteration. The noisy streaks present in the raw reconstructed correction image are removed by the *smoothstep* function plotted on the right. The smooth apodization prevents the accumulation of numerical errors in the corrected image. The window width of difference images is 100 HU.

its quality. Note that the decomposition of differences is a mandatory step that leads to convergence to a corrected image. If one simply reconstructs the difference projections, the negative errors counterbalance the positive errors and the result is an empty image, filled with zero values.

This work considers parallel-beam geometry for which exact analytical image reconstruction is possible for circular trajectories. The aim is to distinguish the reconstruction artifacts due to patient's motion from the possible cone-beam artifacts that are typically introduced by the approximate FDK (Ref. 23) reconstruction method. For application in cone-beam geometry, the method can be combined naturally with the related approach of two-pass correction of cone-beam artifacts.[20] The assessment of image improvements with cone-beam geometry will be tackled in future work.

II.A. Notations

Consider P, the set of projections acquired for a full circular trajectory. The reconstruction from P gives the initial image $I_0 = fbp(P)$, where $fbp(\cdot)$ is the filtered-backprojection[1] (FBP) image reconstruction operator. If the projections P are inconsistent, then the reconstructed image I_0 is corrupted by artifacts and the forward projections $P_0 = fp(I_0)$ do not match the acquired data P. The forward projection operator $fp(\cdot)$ is the inverse of the image reconstruction operator $fbp(\cdot)$.

The set of difference projections $D_0 = P - P_0$ is computed and differences are decomposed into a positive part D_0^+ and a negative part D_0^- such that $D_0 = D_0^+ + D_0^-$ and two correction images $C_0^+ = fbp(D_0^+)$ and $C_0^- = fbp(D_0^-)$ are reconstructed

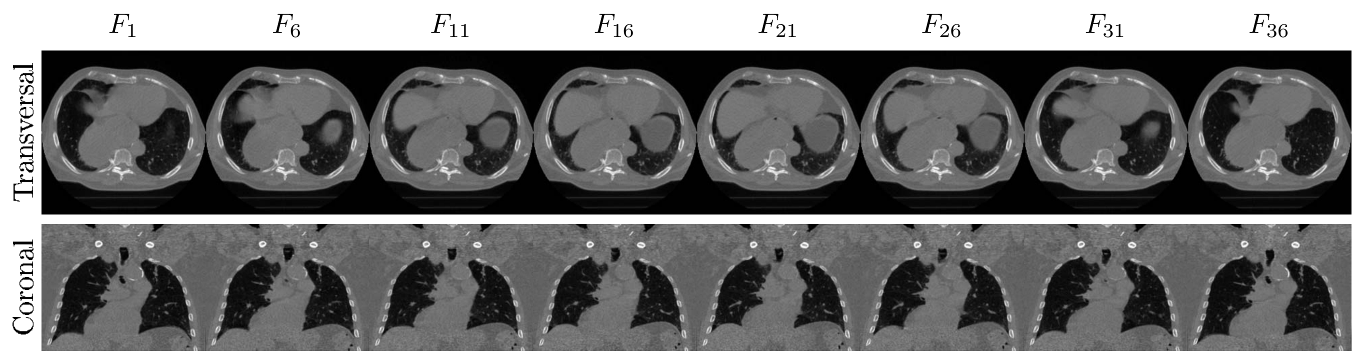

FIG. 4. Transversal slice number 40 and central coronal views of the selected frames 1, 6, 11, 16, 21, 26, 31, and 36 of a respiratory-gated helical CT acquisition. The study covered an axial length of 27 cm with a 35 cm FOV. The first four and second four columns correspond to inhalation and exhalation, respectively. Pulled by contraction of the thoracic diaphragm, organs move out of the selected slice during inhalation.

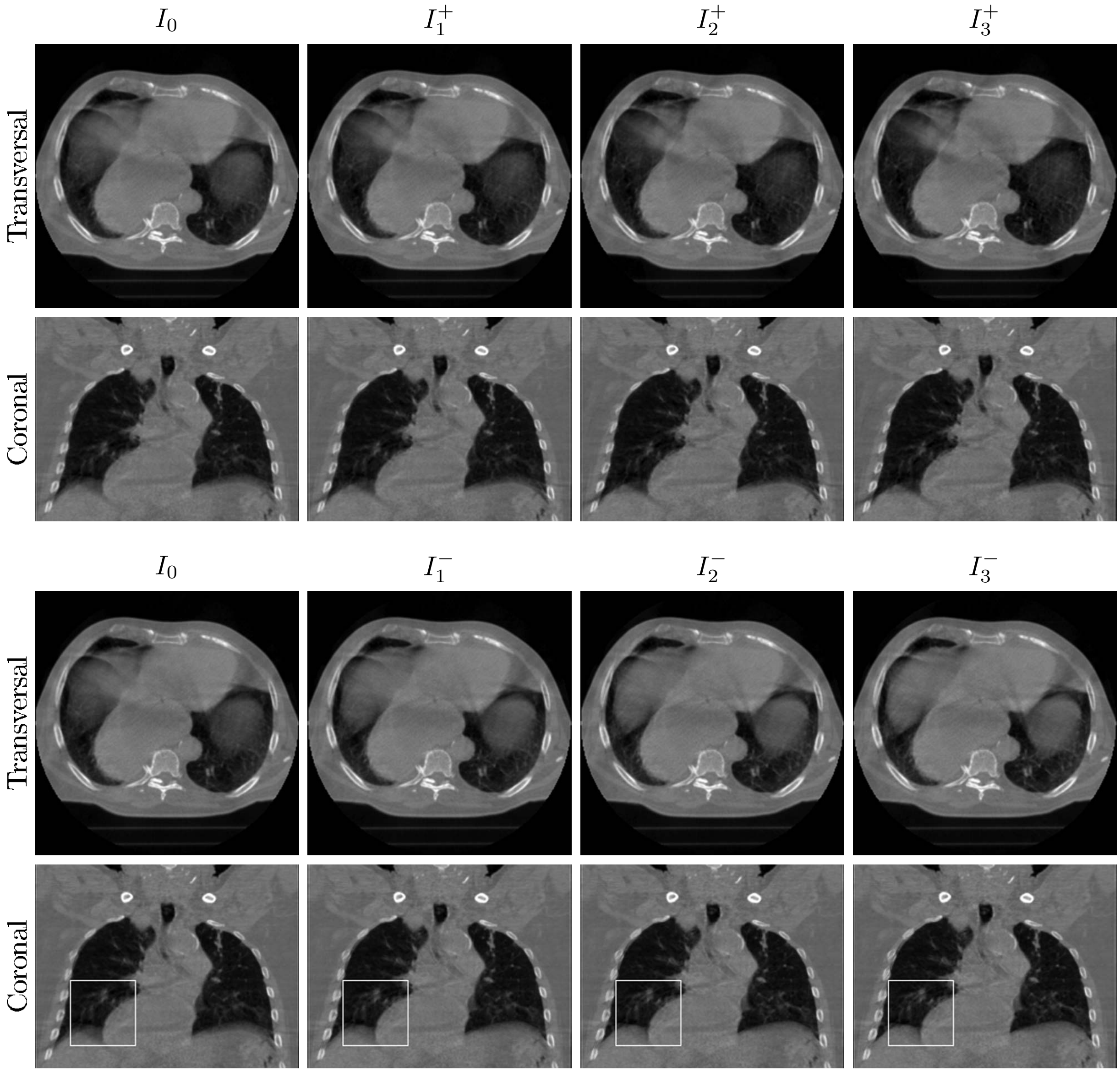

FIG. 5. Transversal slice number 40 and coronal central views of the initial FBP reconstruction and the corrected images after one, two, and three iterations. In the first two rows, the corrected image converges toward the motion state at begin-inhale (end-exhale) when correcting with the positive part of differences. In the last two rows, the corrected image converges toward the motion state at end-inhale (begin-exhale) when correcting with the negative part of differences. The white squares show boundaries of the close-up views shown in Fig. 6.

from each part of the decomposition. Figure 1 shows the decomposition of the line integrals differences for a typical pair of projections.

The images C_0^+ and C_0^- are approximations of the reconstruction artifacts due to, respectively, over- and underestimation of line integrals when reconstructing an image from the acquired data P. The reconstructed artifacts C_0^+ or C_0^- can be subtracted in image space from the initial image I_0, giving the corrected images $I_1^+=I_0-C_0^+$ and $I_1^-=I_0-C_0^-$. Note that even if the decomposed part of line integral differences are all positive or negative, the reconstructed correction images can contain both positive and negative values.

The correction scheme is iterated, while considering either I_1^+ or I_1^- as initial image and improving the correction by reconstructing and subtracting a new correction image C_1^+ or C_1^-. A partially corrected initial image provides a more reliable reference of an artifact-free reconstruction and the estimation of the remaining artifacts will be improved. The two suites of corrected images are $I_{i+1}^+=I_i-C_i^+$ and $I_{i+1}^-=I_i-C_i^-$, with $i\geqslant 0$. The method is a generalization of regular image reconstruction algorithms since the initial image is reconstructed from the acquired data without any compensation.

It is interesting to observe that $fbp(P)=fbp(P_0)=I_0$, so up to numerical inaccuracies, the two sets of projections P and P_0 reconstruct the very same image, although $P\neq P_0$. Furthermore, P_0 is always a consistent set of reference projections but the acquired projections P are consistent only if the inverse of the reconstruction exactly matches the acquired data, hence if $D_0=0$. If the acquired projections P are inconsistent, then $D_0\neq 0$ but still $fbp(D_0)=0$.

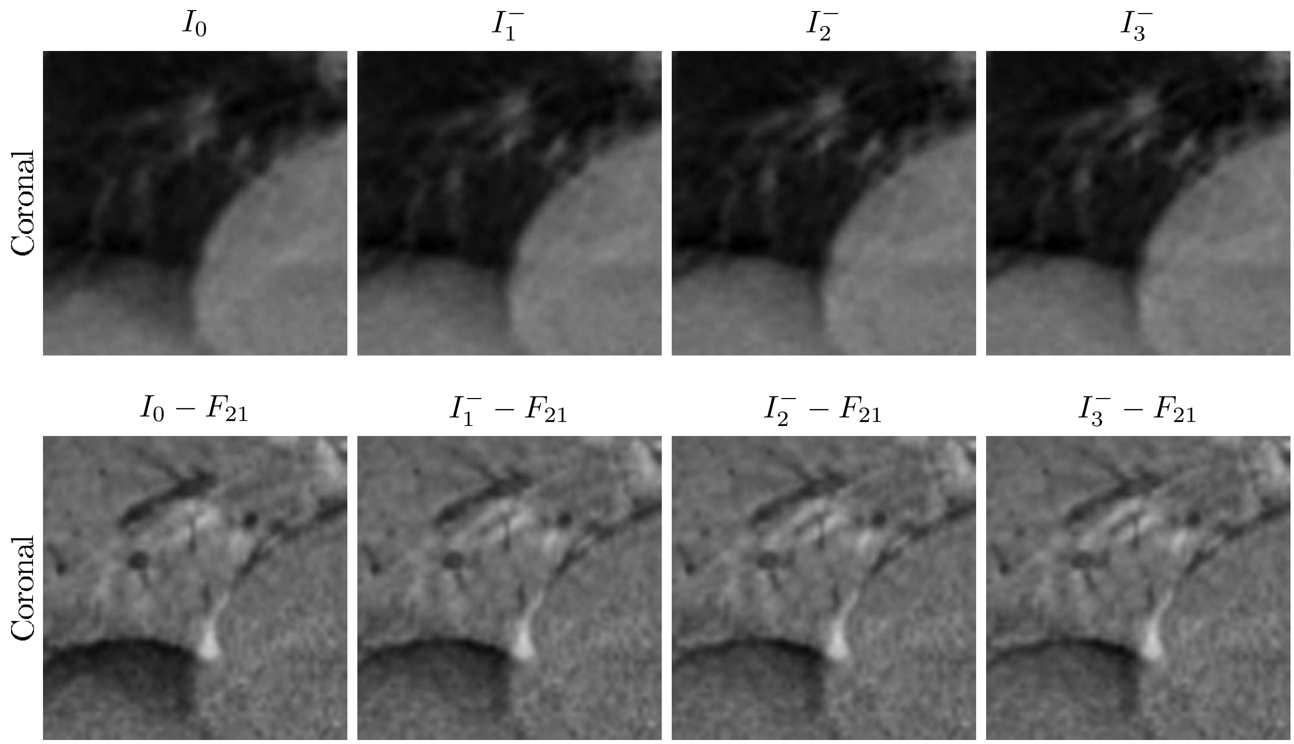

FIG. 6. Close-up views of 64×64 pixels showing the diaphragm border in coronal central views of the initial FBP reconstruction and the corrected images after one, two, and three iterations. Those views are extracted from images in Fig. 5. When correcting with the negative part of differences, the motion blur artifacts are progressively removed as shown by the difference images of the second row. The reference frame F_{21} comes from the dynamic phantom shown in Fig. 4. Since the patient motion is represented by 40 successive images, frame 21 corresponds to the time point in the middle of the respiratory cycle.

II.B. Accuracy issues

The central idea of the method is that the perceived motion is isolated in projection space by computing the difference between the acquired data and the reference data, sampled from a previously reconstructed image. The differences are decomposed and reconstructed by a standard FBP method. The reconstruction uses the very same geometry as the acquired data to obtain an image that is perfectly registered with the initial reconstruction. Unfortunately, the accuracy of the reconstructed motion artifacts is limited by two main factors explained below.

First, the forward projection operation that inverses the image reconstruction operation is implemented by sampling line integrals through a digital image and so the accuracy of the line integral calculation depends on the image interpolation method. Inaccurate image interpolation will introduce aliasing and smoothing or ringing artifacts in the correction images.[24]

Second, the images are reconstructed from a finite number of projections and this inevitably introduces small numerical inaccuracies and streaks in image space. Moreover, the set of the acquired line integrals is not guaranteed to be consistent

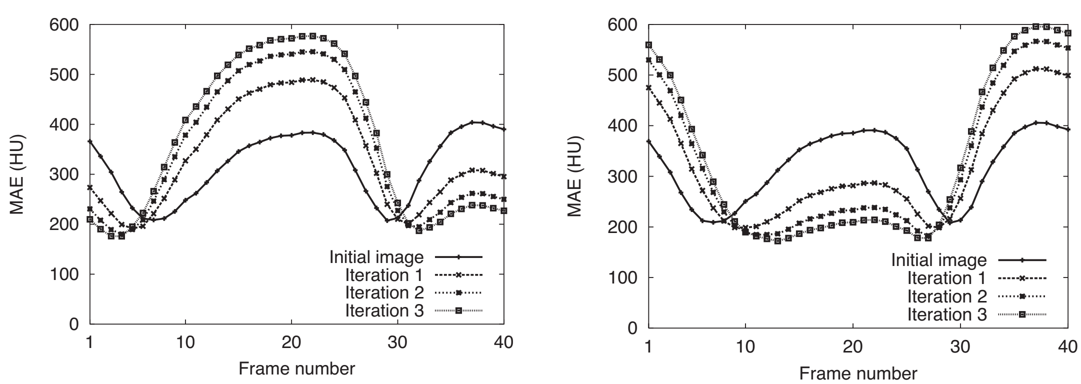

FIG. 7. Quantitative analyses of images for the initial FBP reconstructed image and corrected images after one, two, and three iterations when the correction is applied from the positive (left) and negative (right) part of the decomposed differences. The plots show the MAE in HU between the reconstructed image and each of the original 40 gates shown in Fig. 4. The analysis considers only voxels in regions significantly compensated after the first iteration.

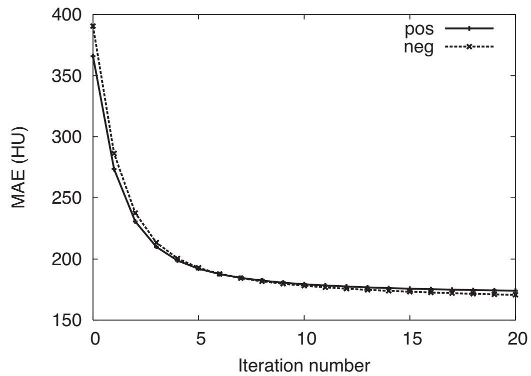

FIG. 8. Analysis of the convergence toward one specific motion state. The "pos" curve plots the MAE in HU between F_1 and the corrected image I_i^+ obtained after iteration $i \in [0,20]$. The reference frame F_1 corresponds to the motion state at the beginning of exhalation. The "neg" curve plots the MAE between F_{21} and the corrected image I_i^- obtained after iteration $i \in [0,20]$. The reference frame F_{21} corresponds to the motion state at the beginning of inhalation. In both cases, a reduction of 50% in terms of the mean absolute error can be observed already after the fourth iteration.

and so the differences can be inconsistent too. Therefore, large streaks might appear in the reconstruction of the correction image itself.

To improve the accuracy of forward projections, the implementation of image interpolation relies on cubic B-spline interpolation, as suggested by Thevenaz *et al.*[25] This method has been demonstrated to limit significantly both aliasing and smoothing, in comparison to the classical linear and cubic interpolation schemes. The impact on image sharpness when using the higher order cubic B-spline interpolation instead of the simpler linear interpolation during forward projections can be seen in Fig. 2.

In addition, the residual numerical errors are eliminated by smoothly apodizing the reconstructed values that are close to zero in the correction images. This regularization leaves the sharp static parts of the initial image untouched, yielding local correction of reconstruction artifacts. The apodization is implemented by multiplying the values of the correction images with the *smoothstep* function defined by

$$smoothstep(a,b,t) = \begin{cases} 0 & \text{if } t < a \\ 1 & \text{if } t > b \\ 3x^2 - 2x^3, x = (t-a)/(b-a) & \text{otherwise,} \end{cases}$$

where $a=0$ Hounsfield units (HU) and $b=30$ HU in the experiments and the parameter t is set to the absolute value of image elements.

In fact, the *smoothstep* function interpolates smoothly between 0 and 1 with a cubic Hermite polynomial. A plot of the interpolation curve and a demonstration of the benefit of the apodization on the quality of a reconstructed correction image can be seen in Fig. 3.

The optimal choice for the threshold b can be evaluated experimentally. Indeed, if no motion occurs during acquisition, the forward projections of the reconstructed image should match the acquired projections, hence the differences should be equal to zero in ideal case. However, the differences are not zero, in practice, because the reconstruction uses a limited number of projections and various discretization as well as numerical errors are transferred to the sampled projections. By measuring the standard deviation of the error distribution, a suitable value for b can be chosen in a principled way.

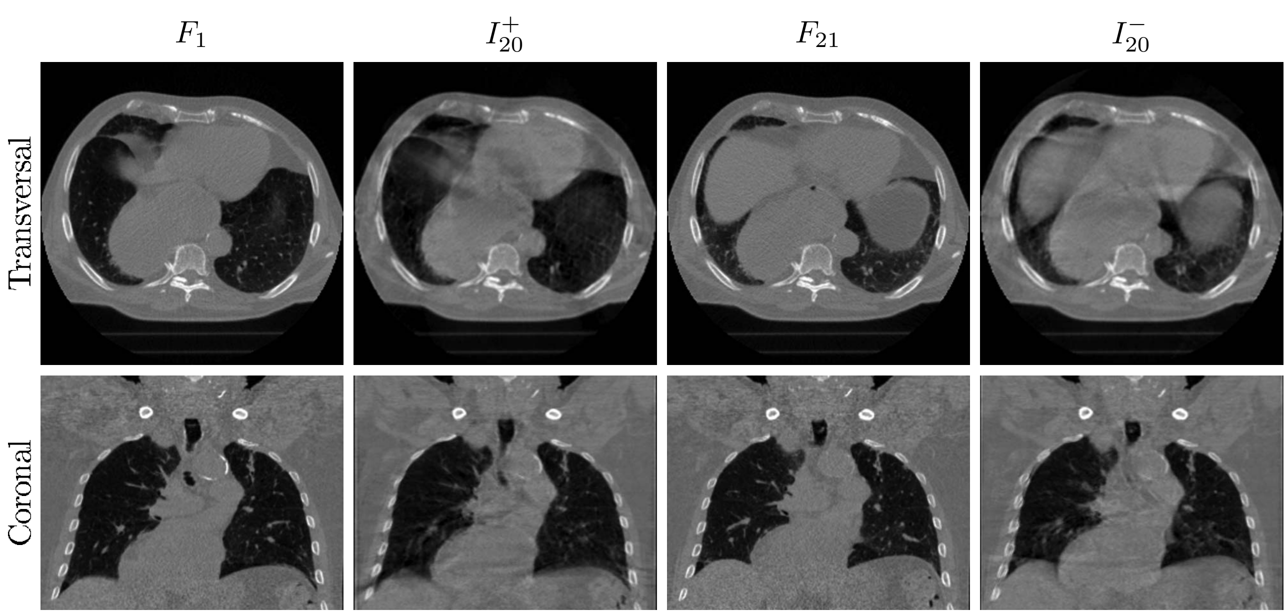

FIG. 9. Side-by-side comparisons of the two possible image correction scenarios. The corrected images are shown after 20 iterations of the iterative motion compensation framework. As suggested by the analyses in Fig. 7, the images get closer to one of the two extreme motion states: The beginning of exhalation (F_1) where the diaphragm is low or the beginning of inhalation (F_{21}) where the diaphragm is high.

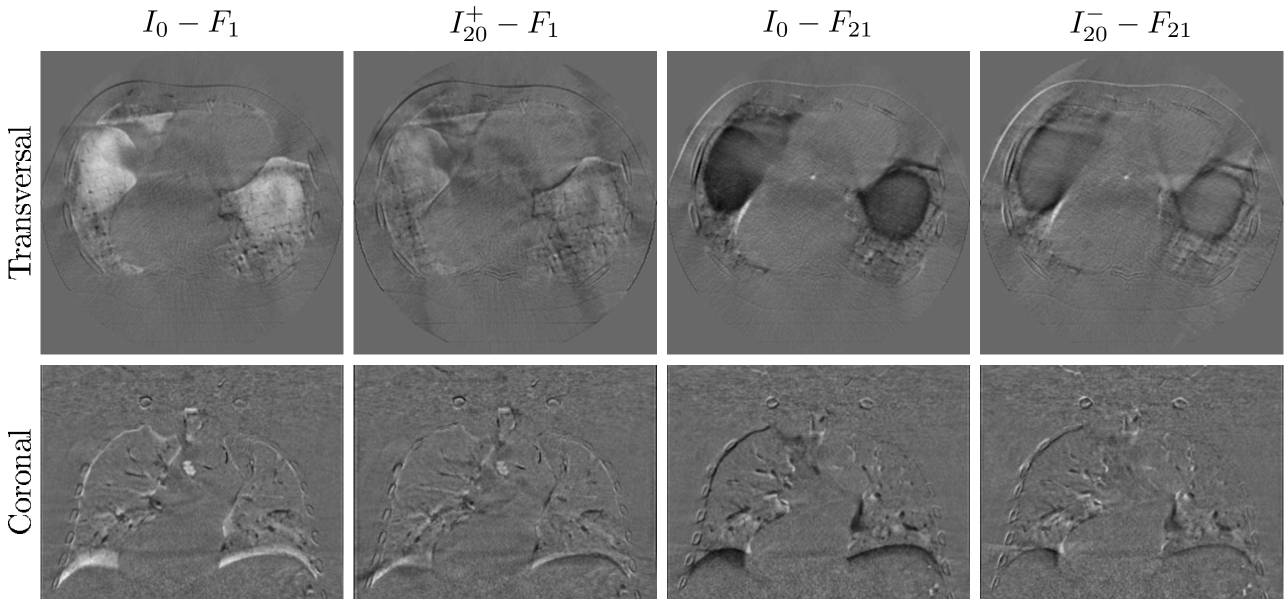

FIG. 10. Transversal slice number 40 and coronal central views of the two selected frames F_1 and F_{21} of the dynamic phantom compared to the initial FBP image I_0 and the two corrected images I_{20}^{+} and I_{20}^{-} obtained after 20 iterations. F_1 corresponds to the start of exhalation (full inspiration) motion state. F_{21} corresponds to the other extreme start of inhalation (full exhalation) motion state. The differences are significantly reduced with motion compensation.

III. RESULTS

In this paper, all slices are extracted from volumetric images represented by a Cartesian grid of $256\times256\times198$ isotropic voxels of size equal to 1.36 mm. Black is set to the attenuation of air and the window width equals 2000 HU such that gray corresponds to the attenuation of water. The window of difference images is centered to zero and the window width is also set to 2000 HU.

To simulate a motion-corrupted acquisition, a set of 1024 parallel-beam projections was numerically simulated from a dynamic free-breathing phantom for one full rotation with a circular trajectory. Experiments consider parallel-beam geometry for which exact analytical image reconstruction is possible for circular trajectories. Since the technique is independent of the specific detector geometry and source trajectory, it can be applied on fan-beam geometry without any change. However, a parallel-beam setup has been preferred because a previous implementation was available and image reconstruction in this simpler geometry suffers less from typical aliasing artifacts that arise in divergent ray geometries.

The forward projection relies on the approximation of line integrals through the digital image using a fast ray-tracing algorithm.[26] The acquisition time was 12 s, matching the typical rotation speed of a C-arm system. This experiment validates the method on a worst case scenario when the patient moves during the whole acquisition instead of holding the breath. Although the simulated breathing motion is naturally periodic, only about 3 cycles can be observed for 12 s.

Selected transversal and coronal slices from the dynamic phantom are shown in Fig. 4. The phantom is based on a sequence of 40 frames reconstructed from a respiratory-gated helical CT acquisition. The speed of the CT gantry was 0.444 s per rotation. The duration of the acquisition was 93.3 s during which 26 breathing cycles were observed. The mean time per cycle was 3.6 s. Images still contain some blurring due to helical artifacts and residual motion within each gate of the breathing cycle.

The initial FBP reconstruction and the corrected images after one, two, and three iterations are shown in Fig. 5. The strong reconstruction artifacts due to inconsistencies among projections can be seen in the initial FBP images of the first column. The liver and stomach appear to be semitransparent in the transversal view. As can be seen in the selected close-up window in Fig. 6, the resolution is limited by strong blurring. When using motion correction, the image quality improves progressively with the number of iterations for some of the frames of the dynamic phantom.

Figure 7 shows quantitative analyses of the reconstructed volumetric image. As the number of iterations increases, the algorithm converges to a particular motion state. The mean absolute error (MAE) with respect to frames close to this optimum motion state decreases with the number of iterations. The plots in Fig. 8 demonstrate the early convergence of the method. After only four iterations, a significant improvement in mean absolute error of over 50% can be appreciated. The analyses only consider voxels that belongs to a region of interest (ROI) which is the collection of voxels that are significantly compensated after the first iteration. A voxel belongs to the ROI if its absolute value of correction exceeds 100 HU.

One of the two extreme motion states (where the diaphragm is the lower or the highest) is selected as an asymptotic state of the iterative framework. The convergence depends on the choice of the positive or negative part of the difference projections. Indeed, when the diaphragm is low (high), then the lungs are filled (empty) and the total mass of the reconstructed image is minimized (maximized). In Fig. 9, side-by-side comparisons of images obtained after convergence (after 20 iterations) illustrate the end results of the experiment with the two possible image correction scenarios. Image quality improvements can be assessed visually from the difference images in Fig. 10.

IV. CONCLUSION

This paper presents a novel compensation algorithm for artifacts due to inconsistencies among projections in static tomographic image reconstruction. The performance of the method is assessed for correction of motion artifacts resulting from a simulated free-breathing acquisition with a slow circular trajectory. In contrast to existing approaches, the projection data are left untouched and the time-dependent deformation is not explicitly modelled, nor estimated. Instead, the perceived motion is extracted in projection space from the difference between the acquired and the reference projections, sampled from the image reconstructed in a previous iteration step. Then, the artifacts are reconstructed in image space and subtracted from an initial reconstruction.

Data inconsistencies are assumed to be caused by organ motion and the reconstruction of artifacts is progressively refined by the iterative scheme. Since no periodicity of the motion is assumed, the technique could also be applied on breath-hold acquisitions to compensate for unstructured movements such as digestive contractions, breath-hold failures, or nervous shaking. Compensation for those kinds of movements may provide a way to further improve the quality of soft tissue images with slowly rotating CT devices, such as interventional C-arm or x-ray imaging systems mounted on linear accelerators for radiotherapy.

ACKNOWLEDGMENTS

The authors thank Thomas Köhler for providing the respiratory-gated image sequence. One of the authors (Colas Schretter) is granted with financial support from the Marie Curie early stage training program of the European Commission under Contract No. MEST-CT-2005-020424.

[a]Author to whom correspondence should be addressed. Electronic mail: colas.schretter@philips.com

[1]A. Kak and M. Slaney, *Principles of Computerized Tomographic Imaging* (IEEE, New York, 1988).
[2]D. Jaffray and J. Siewerdsen, "Cone-beam computed tomography with a flat-panel imager: Initial performance characterization," Med. Phys. **27**(6), 1311–1323 (2000).
[3]C. Ritchie, D. Goodwin, C. Crawford, W. Stanford, H. Anno, and Y. Kim, "Minimum scan speeds for suppression of motion artifacts in CT," Radiology **185**(1), 37–42 (1992).
[4]P. Willis and Y. Bresler, "Optimal scan for time-varying tomography. I. Theoretical analysis and fundamental limitations," IEEE Trans. Med. Imaging **4**(5), 642–653 (1995).
[5]P. Willis and Y. Bresler, "Optimal scan for time-varying tomography. II. Efficient design and experimental validation," IEEE Trans. Med. Imaging **4**(5), 654–666 (1995).
[6]S. Vedam, P. Keall, V. Kini, H. Mostafavi, H. Shukla, and R. Mohan, "Acquiring a four-dimensional computed tomography dataset using an external respiratory signal," Phys. Med. Biol. **48**(1), 45–62 (2003).
[7]J. Sonke, L. Zijp, P. Remeijer, and M. van Herk, "Respiratory correlated cone beam CT," Med. Phys. **32**(4), 1176–86 (2005).
[8]C. Ritchie, C. Crawford, J. Godwin, and K. King, "Correction of computed tomography motion artifacts using pixel-specific back-projection," IEEE Trans. Med. Imaging **15**(3), 333–342 (1996).
[9]S. Roux, L. Desbat, A. Koenig, and P. Grangeat, "Exact reconstruction in 2D dynamic CT: Compensation of time-dependent affine deformations," Phys. Med. Biol. **49**(11), 2169–2182 (2004).
[10]L. Desbat, S. Roux, and P. Grangeat, "Compensation of some time dependent deformations in tomography," IEEE Trans. Med. Imaging **26**(2), 261–269 (2007).
[11]A. Katsevich, "Motion compensated local tomography," Inverse Probl. **24**(4), 45012–45021 (2008).
[12]T. Li, L. Xing, P. Munro, C. McGuinness, M. Chao, Y. Yang, B. Loo, and A. Koong, "Four-dimensional cone-beam computed tomography using an on-board imager," Med. Phys. **33**(10), 3825–3833 (2006).
[13]R. Zeng, J. Fessler, and J. Balter, "Estimating 3-D respiratory motion from orbiting views by tomographic image registration," IEEE Trans. Med. Imaging **26**(2), 153–163 (2007).
[14]W. Lu and T. Mackie, "Tomographic motion detection and correction directly in sinogram space," Phys. Med. Biol. **47**(8), 1267–1284 (2002).
[15]S. Leng, B. Nett, M. Speidel, and G. Chen, "Motion artifact reduction in fan-beam and cone-beam computed tomography via the fan-beam data consistency condition (FDCC)," Proc. SPIE **6510**, 6510–6511W (2007).
[16]H. Yu, Y. Wei, J. Hsieh, and G. Wang, "Data consistency based translational motion artifact reduction in fan-beam CT," IEEE Trans. Med. Imaging **25**(6), 792–803 (2006).
[17]H. Yu and G. Wang, "Data consistency based rigid motion artifact reduction in fan-beam CT," IEEE Trans. Med. Imaging **26**(2), 249–260 (2007).
[18]M. Unser, "Sampling—50 years after shannon," Proc. IEEE **88**(4), 569–587 (2000).
[19]D. Jaffray *et al.*, "Flat-panel cone-beam computed tomography for image-guided radiation therapy," Int. J. Radiat. Oncol., Biol., Phys. **53**(5), 1337–1349 (2002).
[20]J. Hsieh, "Two-pass algorithm for cone beam reconstruction," Proc. SPIE **3979**, 533–540 (2000).
[21]W.-T. Lin, "A motion compensation algorithm for arbitrary translation of CT objects," Proc. SPIE **2167**, 743–754 (1994).
[22]N. Linney and P. Gregson, "Organ motion detection in CT images using opposite rays in fan-beam projection systems," IEEE Trans. Med. Imaging **20**(11), 1109–1122 (2001).
[23]L. Feldkamp, L. Davis, and J. Kress, "Practical cone-beam algorithm," J. Opt. Soc. Am. **1**(6), 612–619 (1984).
[24]F. Xu and K. Mueller, "A comparative study of popular interpolation and integration methods for use in computed tomography," *Proceedings of IEEE International Symposium on Biomedical Imaging*, 2006 (unpublished).
[25]P. Thevenaz, T. Blu, and M. Unser, "Interpolation revisited," IEEE Trans. Med. Imaging **19**(7), 739–758 (2000).
[26]C. Schretter, "A fast tube of response ray-tracer," Med. Phys. **33**(12), 4744–4748 (2006).